International Journal of Pharmaceutics 393 (2010) 253–262

Contents lists available at ScienceDirect

International Journal of Pharmaceutics

journal homepage: www.elsevier.com/locate/ijpharm

Pharmaceutical Nanotechnology

Photosensitizer loaded HSA nanoparticles. I: Preparation and photophysical properties

Matthias Wacker[a], Kuan Chen[b], Annegret Preuss[b], Karin Possemeyer[c], Beate Roeder[b], Klaus Langer[c,*]

[a] Institute of Pharmaceutical Technology, Biocenter of Goethe-University, D-60438 Frankfurt, Germany
[b] Institute of Physics, Humboldt-Universität zu Berlin, D-12489 Berlin, Germany
[c] Institute of Pharmaceutical Technology and Biopharmacy, Westfälische Wilhelms-Universität, Corrensstrasse 1, D-48149 Münster, Germany

ARTICLE INFO

Article history:
Received 4 January 2010
Received in revised form 12 April 2010
Accepted 17 April 2010
Available online 24 April 2010

Keywords:
Photosensitization
Drug adsorption
Nanoparticles
Human serum albumin
Singlet oxygen

ABSTRACT

Photodynamic therapy (PDT) is a promising option in the treatment of cancer. Efficient photosensitizers are available but many of them have insufficient physico-chemical properties for parenteral application. We have established nanoparticles consisting of human serum albumin (HSA) as a drug carrier system for 5,10,15,20-tetrakis(*m*-hydroxyphenyl)porphyrine (mTHPP) and 5,10,15,20-tertrakis(*m*-hydroxyphenyl)chlorin (mTHPC), two well-known photosensitizers.

Nanoparticle loading was performed in water/ethanol mixtures in the presence of dissolved HSA acting as solubilizer for photosensitizers. The HSA concentration was optimized to exclude precipitation in the nanoparticle suspension and to increase binding to nanoparticles. Additionally, the influence of pH and incubation time on drug adsorption was investigated. A freeze drying method was established for mTHPC loaded nanoparticles and the storage stability of the freeze dried formulation was tested.

PDT related photophysical parameters of drug loaded HSA nanoparticles, especially singlet oxygen generation, are presented. Both preparations were able to generate singlet oxygen with low quantum yield. In contrast, efficient singlet oxygen generation was obtained when Jurkat cells were incubated with mTHPP and mTHPC loaded HSA nanoparticles. This indicates that the photosensitizer molecules were successfully released from the nanoparticles that were taken up by the cells. Therefore, the efficiency of HSA nanoparticles as drug carriers for photosensitizers was proven under *in vitro* conditions.

1. Introduction

Photodynamic therapy (PDT) is a treatment option for several diseases. It is based on the illumination of a photosensitizer with visible or infrared light in the presence of oxygen. These drugs with photosensitizing properties are of no or low dark toxicity. Absorption of light with suitable wavelength by the tumour-localized sensitizer molecules leads to the generation of singlet oxygen, which directly or indirectly destroys tumour tissue.

The pathways of localized tumour destruction are still under investigation but both cell killing mechanisms, apoptosis and necrosis, are described (Oleinick et al., 2002). Within a few hours after successful PDT tumour tissue exhibits extensive regions of necrosis and apoptosis. Additionally, inflammatory and immune responses are induced by PDT (Brown et al., 2004).

Tumour destruction can be realized by both, cell death and photodestruction of the tumour vasculature resulting in local hypoxia and indirect cell death (Henderson and Dougherty, 1992; Dougherty et al., 1998). Targeting the vasculature can also starve tumours by cutting oxygen-carrying blood supply. Because of their low selectivity for the malignant tissues high doses of photosensitizers are needed to reach therapeutic concentrations and to induce an apoptotic process in tumour cells. Colloidal drug delivery systems are well suited as an efficient strategy to circumvent resulting side effects of a conventional photosensitizer therapy. The drug loading to nanoparticles may reduce the precipitation of the lipophilic photosensitizer at the site of injection. Furthermore, the modification of the body distribution by nanoparticles will help to avoid damage on normal tissues triggered by light exposure or self-activation of the photosensitizer (Bourdon et al., 2002; Moreno-Aspitia and Perez, 2005; Zeisser-Labouebe et al., 2006).

It was the aim of the present study to evaluate human serum albumin (HSA) nanoparticles as drug carriers for the photosensitizers mTHPP and mTHPC. The drugs were adsorbed to preformed HSA nanoparticles. In principle, drugs can be incorporated within the particle matrix, adsorbed onto the particle surface or bound by covalent linkage. An advantage of the adsorptive binding can be seen in a fast drug release from the carrier leading to a high activity in terms of photosensitization. As it is well known that the monomeric form of porphyrin derivatives can be stabilized in albumin solutions (Sasnouski et al., 2005) drug adsorption was

* Corresponding author. Tel.: +49 251 83 39860; fax: +49 251 83 39308.
E-mail address: k.langer@uni-muenster.de (K. Langer).

0378-5173/$ – see front matter © 2010 Elsevier B.V. All rights reserved.
doi:10.1016/j.ijpharm.2010.04.022

performed in the presence of dissolved HSA. Under the chosen conditions dissolved HSA served as solubilizer building a stable hydroethanolic solution of the photosensitizers in their monomeric form. Preserving the monomeric drug form is of major importance as this form is responsible for singlet oxygen generation, which results in the photodynamic response (Cramers et al., 2003; Detty et al., 2004).

For photodynamic therapy other polymers for nanoparticle formulations have been evaluated before (Compagnin et al., 2009; Jux and Röder, 2010). In the present study human serum albumin (HSA) was used for the preparation of nanoparticles due to its biodegradability and enhanced uptake in human cancer cells (Kratz, 2008; Miele et al., 2009). HSA nanoparticles in a size range between 150 and 300 nm, as they were used for our adsorption experiments, are well known to accumulate in tumour tissues because of the high permeability of tumour vasculature. This enhanced permeability and retention (EPR) effect was identified by Maeda et al. to describe size-related drug accumulation in tumour tissue (Matsumura and Maeda, 1986; Greish, 2007). Once taken up by endocytosis the nanoparticles are degraded by various enzymes (Langer et al., 2008) and easily release their drug load. The uptake of silica nanoparticles mediated by plasma proteins is known from literature (Compagnin et al., 2009) and it could be anticipated that the new developed albumin nanoparticles show similar effects regarding the efficiency of their uptake and photodynamic activity (Zhao et al., 2009). In comparison to these earlier formulations the stability of HSA nanoparticles in different cell culture media and *in vivo* has been investigated before (Wartlick et al., 2004; Steinhauser et al., 2008; Zensi et al., 2009) and due to their chemically stabilized surface there are no other excipients needed in the final formulation.

The fast release of the photosensitizers as it will be presented in the second part of this study for HSA nanoparticles is a desirable advantage of the chosen material to shorten the interval between administration and illumination of the drug. Otherwise residues of the drug could be released over a longer period of time and cause side effects such as photosensitivity which is a known problem for many of the first-generation photosensitizers (Levy, 1995; D'Cruz et al., 2004). Furthermore patients who were treated with Abraxane®, which is a formulation of paclitaxel containing human serum albumin, showed no acute hypersensitivity reactions or unexpected toxicities. Therefore, HSA nanoparticles are suitable carriers for a specific and compliant therapy with photosensitizers.

2. Materials and methods

2.1. Reagents and chemicals

Human serum albumin (Fraction V), glutaraldehyde 8% aqueous solution, and pepsin (batch 087H0163) were purchased from Sigma (Steinheim, Germany). 5,10,15,20-Tetrakis(*m*-hydroxyphenyl)porphyrin (mTHPP) and 5,10,15,20-tetrakis(*m*-hydroxyphenyl)chlorin (mTHPC) were obtained from Biolitec AG (Jena, Germany). Formic acid was purchased from Merck (Darmstadt, Germany). All reagents were of analytical grade and used as received.

2.2. Solubility of mTHPP and mTHPC in hydroethanolic HSA solution

For the preparation of a HSA stock solution an amount of 100 mg HSA was dissolved in 1 mL of 10 mM sodium chloride solution. The pH was adjusted to 8.0 and the solution was filtered through a 0.22 μm filtration unit (Schleicher und Schüll, Dassel, Germany). Stock solutions of the photosensitizers were prepared by dissolving 1.0 mg of mTHPP or mTHPC in 1 mL ethanol 96.0% (v/v).

An amount of 18.8, 37.5, 56.3, 75.0, 93.8, 112.5, 131.3, and 150.0 μL of the aqueous HSA solution was filled up to a volume of 500.0 μL with purified water. To each mixture 112.5 μL of the photosensitizer stock solution and 137.5 μL of ethanol 96% (v/v) were added resulting in HSA concentrations between 0.25 and 2.0% (m/v). The samples were incubated for 12 h under permanent shaking (660 rpm) followed by centrifugation at 20,817 × *g* over 120 min. Centrifugation and incubation steps were performed at 15 °C to prevent loss of ethanol by evaporation during the preparation process. Before and after incubation and centrifugation 50.0 μL of each mixture were diluted with 450.0 μL ethanol 34.3% (v/v) and were measured photometrically at 512 nm (Hitachi U-3000, Tokyo, Japan) for mTHPP and at 517 nm for mTHPC to quantify the drug content of the photosensitizers before and after incubation. For validation of the method stable ethanolic solutions (75–187.5 μg/mL) of the drugs were measured under comparable conditions. Linearity, precision and accuracy of the photometric measurement were shown for both photosensitizers.

2.3. Preparation of HSA nanoparticles

Human serum albumin (HSA) nanoparticles were prepared by a desolvation method as described previously (Marty et al., 1978; Weber et al., 2000; Langer et al., 2003). In principle, an amount of 100 mg HSA was dissolved in 1 mL 10 mM sodium chloride solution. The pH was adjusted to 8.0 and the solution was filtered through a 0.22 μm filtration unit (Schleicher und Schüll, Dassel, Germany). Nanoparticles were formed by continuous addition of 4.0 mL ethanol under permanent stirring (380 rpm) at room temperature. A pumping device (Ismatec IPN, Glattbrugg, Switzerland) allowed a defined rate of ethanol addition (1 mL/min). After protein desolvation 57.76 μL of 8% aqueous glutaraldehyde solution were added to stabilize the resulting protein nanoparticles by chemical crosslinking. The glutaraldehyde concentration used corresponds to 100% stoichiometric crosslinking of the amino groups in 100 mg HSA. Particles were stirred for 1 h and were purified by 3 cycles of centrifugation (20,817 × *g*, 10 min) and redispersion in 1.0 mL water in an ultrasonic bath (5 min).

2.4. Nanoparticle characterization

Average particle size and polydispersity were measured by photon correlation spectroscopy using a Zetasizer 3000 HSA (Malvern Instruments, Malvern, UK). The nanoparticle content was determined by microgravimetry and was adjusted to 15.0 mg/mL.

2.5. mTHPP and mTHPC loading of HSA nanoparticles in the presence of dissolved HSA

An amount of 100 mg of HSA was dissolved in 1 mL of 10 mM sodium chloride solution. The pH was adjusted to 8.0 and the solution was filtered through a 0.22 μm filtration unit (Schleicher und Schüll, Dassel, Germany). To 333.0 μL of the HSA nanoparticle suspension (15 mg/mL) 56.3, 75.0, 93.8, 112.5, 131.3, and 150.0 μL (0.75–2.0%) of the resulting aqueous HSA solution were added, respectively. The suspensions were adjusted to 500.0 μL with purified water followed by addition of 112.5 μL of an ethanolic photosensitizer stock solution (ethanol 96% (v/v), 1 mg/mL) and 137.5 μL of ethanol 96% (v/v). The samples were incubated for 2 h under permanent shaking (15 °C, 660 rpm). The nanoparticles were purified by repeated centrifugation (15 °C, 20,817 × *g*, 10 min) and redispersion in 1 mL of purified water in an ultrasonic bath (5 min).

During purification after every centrifugation step 50.0 μL of the supernatant were diluted with 950.0 μL ethanol 96% (v/v) and measured photometrically (Hitachi U-3000, Tokyo, Japan) at 512 nm for

mTHPP and at 517 nm for mTHPC in order to detect the unbound photosensitizer. The purification steps were repeated until no photosensitizer was detectable in the supernatant.

For the quantification of drug loading a standard solution of both photosensitizers (water instead of HSA nanoparticles) was incubated under comparable conditions.

2.6. Influence of incubation time and pH value on mTHPP and mTHPC loading

For the determination of the influence of incubation time, the drug loading was performed as described above. All samples were prepared in the presence of 112.5 μL aqueous HSA solution (1.5%) for mTHPP and 150.0 μL aqueous HSA solution (2.0%) for mTHPC. Samples were incubated for 0.5, 1, 2, and 24 h under permanent shaking (15 °C, 660 rpm) followed by purification and characterization.

For the determination of the influence of pH value, the drug loading was performed as described. All samples (mTHPP and mTHPC) were prepared in the presence of 112.5 μL aqueous HSA solution (1.5%) previously adjusted to pH values of 4, 8, and 10, respectively. During nanoparticle purification the pH of the supernatant was measured to determine final pH value of the preparation. The final pH was used for data presentation.

2.7. Direct quantification of particle loading

For the direct quantification of mTHPP and mTHPC loading of nanoparticles 10 mg pepsin were dissolved in 1 mL of an aqueous solution of formic acid 1%. An aliquot containing 1.0 mg photosensitizer loaded HSA nanoparticles was added to 250 μL of the pepsin solution. The mixture was adjusted to 500.0 μL with purified water. The samples were incubated for 2 h under permanent shaking. After incubation 1.0 mL of ethanol 96% (v/v) was added followed by centrifugation of the solution (15 °C, 20,817 × *g*, 30 min). To 800.0 μl of the supernatant an amount of 200.0 μL 50 mM bicarbonate buffer (pH 9) was added. The solution was measured photometrically at 512 nm for mTHPP and 517 nm for mTHPC to determine the content of photosensitizer released after enzymatic nanoparticle degradation.

For quantification standards containing 25 μg of photosensitizer and a control preparation containing 1 mg unloaded HSA nanoparticles were measured under the same conditions.

2.8. Scanning electron microscopy (SEM) of nanoparticles

Nanoparticles were prepared and purified as described above. An amount of 2.0% dissolved HSA was used for mTHPC adsorption. An aliquot of the particle suspension (20 μL) was placed on a membrane filter (Millipore VSWP 0,025 μm, Millipore, Schwalbach, Germany) and was allowed to dry over 4 h in an exsiccator. Membrane filters with nanoparticles were sputtered with gold (Sputter SCD 040, BAL-TEC, Liechtenstein). An aliquot of purified water was handled under the same conditions and was used as a control.

Electron microscopy was performed in a CamScan CS4 microscope system (Cambridge Scanning Company, UK) using an accelerating voltage of 10 kV, a working distance of 10 mm and 20,000-fold magnification using secondary electron detection mode.

2.9. Zeta potential measurements of HSA nanoparticles

The nanoparticles loaded with mTHPP and mTHPC were prepared as described above in the presence of 2.0% (m/v) dissolved HSA for mTHPC and 1.5% (m/v) dissolved HSA for mTHPP. The zeta potential of the colloid system was measured directly after preparation and after a storage time of 1, 2, 3, 4, and 5 days in a Malvern Zetasizer 3000 HSA (Malvern Instruments, Malvern, UK).

2.10. Protein adsorption to HSA nanoparticles

Nanoparticles loaded with mTHPC were prepared as described above. An amount of 2.0% HSA was used for photosensitizer adsorption. After the first centrifugation step the supernatant was analysed for unbound HSA by a previously described size exclusion chromatography (SEC) method (Langer et al., 2008). HSA in purified water and samples containing dissolved HSA and mTHPC but without HSA nanoparticles were measured under comparable conditions.

2.11. Freeze drying of mTHPC loaded HSA nanoparticles

The nanoparticles loaded with mTHPC were prepared as described above. After the addition of 3% (m/v) sucrose to the aqueous suspension containing 5 mg HSA nanoparticles in a volume of 1.0 mL of purified water the freeze drying process was performed in an Christ Epsilon 1-4 freeze dryer (Christ, Osterode, Germany). Samples containing photosensitizer loaded nanoparticles but without the addition of sucrose were used as control. Vials with a maximum volume of 2 mL (Macherey-Nagel, Düren, Germany) were used.

For freeze drying of the samples the shelf temperature was reduced from +20 to −40 °C at a rate of 1 °C/min. These parameters were held for 2 h before the temperature was increased to −30 °C over 30 min. The primary drying was started by evacuation of the freeze drying chamber to a pressure of 1.030 mbar. During this drying process temperature was firstly increased to −15 °C (0.1 °C/min) and then to +20 °C for secondary drying process (0.23 °C/min). These parameters were held for 9.5 h. Afterwards the pressure was reduced to 0.001 mbar and temperature was increased to 30 °C (0.2 °C/min). These parameters were held for 2 h before the freeze drying process was finished.

The freeze dried samples were stored at 20 °C for 1 day, 3 weeks, and 6 weeks. The reconstitution was performed as follows: after addition of 1 mL of purified water the samples were allowed to sit for 5 min to ensure a proper wetting of the lyophilised cake. Afterwards, samples were vortexed (Vortex-Genie 2, Scientific Industries, Inc., Bohemia, NY, USA) for 5 min at maximum vortex speed to ensure complete disintegration of the cake.

The control samples containing an aqueous nanoparticle suspension and the stabilizer sucrose were stored at 4 °C. Average particle size and polydispersity were measured by photon correlation spectroscopy as described previously for both preparations.

2.12. Photophysical characterization in solution

The PDT-associated photophysical properties of two drug loaded HSA nanoparticle samples were tested. Ground state absorption spectra were measured by a spectrophotometer UV-160A (Shimadzu, Japan) at room temperature. Steady-state fluorescence spectra were excited at 516 nm using a Xenon lamp (XBO 150, OSRAM) with a monochromator (LOT-Oriel, France). Fluorescence emission was recorded by a cooled CCD matrix (LOT-Oriel Instaspec IV).

Fluorescence lifetime measurements were carried out using time correlated single photon counting (TCSPC) technique. The samples were excited at 532 nm by a Nd:VO_4 laser (Cougar, Time Bandwidth products). Fluorescence was detected with a cooled microchannel plate (R3809-01, Hamamatsu, Japan) under the magic angle of 54.7°. The fluorescence signal was recorded at 717 nm.

Singlet oxygen luminescence at 1268 nm was detected with a liquid nitrogen-cooled Ge-diode detector Model EO-817P (North Coast, Inc., Santa Rosa, CA). The excitation wavelength was 516 nm. The concentration of all photosensitizers was 8 μM. For mTHPP and mTHPC, singlet oxygen luminescence was measured in ethanol. Pheophorbide a in ethanol (singlet oxygen quantum yield $\Phi_\Delta = 0.52$) was taken as reference (Redmond and Gamlin, 1999). For mTHPP and mTHPC loaded HSA nanoparticles, the singlet oxygen luminescence was measured in D_2O. Rose Bengal in D_2O ($\Phi_\Delta = 0.75$) was taken as reference (Redmond and Gamlin, 1999). The intensity of singlet oxygen luminescence can be calculated using Eq. (1) (Redmond and Gamlin, 1999):

$$I(t) = A \cdot \left[\exp\left(\frac{-t}{\tau_\Delta}\right) - \exp\left(\frac{-t}{\tau_T}\right)\right] \cdot \frac{\tau_\Delta}{\tau_\Delta - \tau_T} \quad (1)$$

where $I(t)$ is the intensity of singlet oxygen luminescence, A is a constant that depends on several setup parameters and on the solvent. It also relates to k_Δ the singlet oxygen luminescence rate constant. τ_Δ is singlet oxygen luminescence lifetime and τ_T is triplet state lifetime of photosensitizer.

2.13. Singlet oxygen detection in living cells

Before measurement, Jurkat cells (clone E 6-1 human acute T-cell leukaemia) were incubated in cell culture medium (RPMI 1640, GIBCO) with 3 μM mTHPP, mTHPP loaded HSA nanoparticles, mTHPC and mTHPC loaded HSA nanoparticles for 5 h, respectively, following the procedure described in Rancan et al. (2005). After 5 h incubation, the cells were harvested and counted (about 2×10^5 cells/mL). The cells were washed with PBS after centrifugation (room temperature, 350 × *g*, 5 min).

A newly built time-resolved singlet oxygen luminescence detection setup based on Time Correlated Multi Photon Counting (TCMPC) technique was used for singlet oxygen luminescence detection in living cells (Schlothauer et al., 2008). For excitation a Nd:YAG laser (Coherent) and a YAG-pumped dye laser was used. The excitation wavelengths were 532 nm for mTHPP and mTHPP loaded HSA nanoparticles and 650 nm for mTHPC and mTHPC loaded HSA nanoparticles, respectively. The average irradiation power was 500 μW.

3. Results

In the present study the preparation of human serum albumin (HSA) nanoparticles as drug carrier systems for the highly potent photosensitizers mTHPP and mTHPC was established. Adsorptive drug loading was performed in the presence of dissolved HSA as solubilizer in order to prevent aggregation of the lipophilic molecules.

PDT-associated photophysical properties of mTHPP loaded and mTHPC loaded HSA nanoparticles are presented. The singlet oxygen generation of drug loaded HSA nanoparticles in solution and in Jurkat cells was evaluated as well.

3.1. Solubility of mTHPP and mTHPC in hydroethanolic HSA solution

In order to prevent precipitation of mTHPP and mTHPC during adsorptive drug loading to HSA nanoparticles and to optimize the content of dissolved HSA in the hydroethanolic loading mixture, a solubility study of mTHPP and mTHPC was performed. Increasing concentrations of dissolved HSA in the range of 0–2.0% (m/v) were combined with 0.15 mg/mL photosensitizer in 34.3% (v/v) ethanol/water mixture. Recovery of mTHPP and mTHPC was determined photometrically (512 nm for mTHPP and 517 nm for mTHPC) before and after 12 h incubation of the samples (Fig. 1). A minimum concentration of 0.5% HSA was necessary to stabilize both photosensitizer solutions over 12 h. At this and higher HSA concentrations a 100% recovery of mTHPP and mTHPC in soluble form without any signs of drug precipitation was achieved.

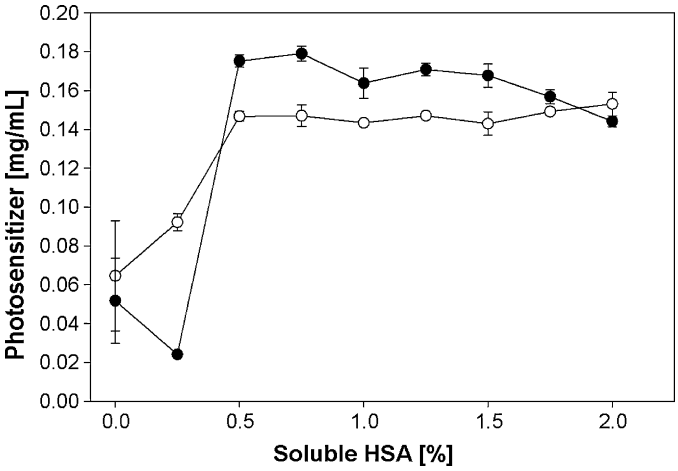

Fig. 1. Solubility of mTHPP (○) and mTHPC (●) in hydroethanolic reaction mixture containing 0.15 mg/mL photosensitizer in ethanol 34.3% (v/v) depending on the concentration of dissolved HSA (0.25, 0.5, 0.75, 1.0, 1.25, 1.5, 1.75, and 2.0%) after 12 h incubation. Stable mTHPP and mTHPC solutions were achieved for HSA concentrations >0.5% (mean ± S.D.; $n = 3$).

3.2. Preparation of HSA nanoparticles

Human serum albumin (HSA) nanoparticles were prepared by a well established desolvation procedure (Marty et al., 1978; Weber et al., 2000; Langer et al., 2003). Particle formulations were chemically stabilized with glutaraldehyde concentrations corresponding to a 100% stoichiometric crosslinking of the amino groups in the HSA molecule. After purification HSA nanoparticles for drug loading with photosensitizer were obtained. Nanoparticles for loading with mTHPP showed a particle diameter of 189.9 ± 0.4 nm. A polydispersity index of 0.045 ± 0.024 ($n = 6$) indicated monodisperse size distribution (Table 1). HSA nanoparticles for mTHPC loading procedure showed a particle diameter of 211.6 ± 5.7 nm and a polydispersity index of 0.038 ± 0.008 (Table 2).

For further drug loading experiments HSA nanoparticles were diluted with purified water to a particle content of 15.0 mg/mL.

3.3. Photosensitizer loading of HSA nanoparticles in the presence of dissolved HSA

Based on the solubility results of mTHPP and mTHPC solutions drug loading was performed in mixtures containing 0.15 mg/mL of the photosensitizer and 6.67 mg/mL HSA nanoparticles in 34.3% (v/v) ethanol. Dissolved HSA was added in concentrations between 0.75 and 2.0% (m/v) which were found to stabilize the solutions of both photosensitizers. Particle loading with mTHPP and mTHPC in the presence of increasing HSA concentrations showed no significant influence on particle size and size distribution. Independent of the HSA concentration a particle diameter between 194.7 and 204.0 nm with polydispersity indices between 0.009 and 0.086 was observed for mTHPP loaded nanoparticles (Table 1) and a particle diameter between 199.0 and 208.2 nm with polydispersity indices between 0.006 and 0.081 for mTHPC loaded nanoparticles (Table 2). The polydispersity indices indicated a monodisperse size distribution for all formulations.

Photosensitizer loading was quantified after enzymatic degradation of the nanoparticles. With increasing concentrations of dissolved HSA between 0.75 and 2.0% a slight but not significant (ANOVA) decrease of mTHPP loading from 21.6 to 17.3 μg/mg was

Table 1
Physico-chemical characteristics of mTHPP loaded HSA nanoparticles in the presence of increasing amounts of dissolved HSA used as solubilizer (mean ± S.D.; $n = 6$).

Parameter	Unloaded	0.75% HSA	1.0% HSA	1.25% HSA	1.5% HSA	1.75% HSA	2.0% HSA
Particle diameter [nm]	189.9 ± 0.4	194.7 ± 6.4	197.0 ± 5.0	195.6 ± 3.0	204.0 ± 5.2	199.7 ± 14.3	203.0 ± 18.0
Polydispersity	0.045 ± 0.024	0.050 ± 0.001	0.026 ± 0.011	0.064 ± 0.016	0.009 ± 0.009	0.069 ± 0.009	0.086 ± 0.082
mTHPP loading [μg/mg]	–	21.6 ± 6.8	21.0 ± 7.0	21.1 ± 0.2	20.3 ± 1.0	18.6 ± 0.2	17.3 ± 0.3

Table 2
Physico-chemical characteristics of mTHPC loaded HSA nanoparticles in the presence of increasing amounts of dissolved HSA used as solubilizer (mean ± S.D.; $n = 3$).

Parameter	Unloaded	0.75% HSA	1.0% HSA	1.25% HSA	1.5% HSA	1.75% HSA	2.0% HSA
Particle diameter [nm]	211.6 ± 5.7	200.4 ± 0.9	199.6 ± 0.8	199.0 ± 1.8	203.2 ± 2.2	208.2 ± 2.7	206.9 ± 3.6
Polydispersity	0.038 ± 0.008	0.043 ± 0.018	0.006 ± 0.004	0.044 ± 0.012	0.055 ± 0.018	0.016 ± 0.010	0.081 ± 0.062
mTHPC loading [μg/mg]	–	24.1 ± 0.5	25.2 ± 0.5	21.7 ± 1.9	23.2 ± 0.8	21.4 ± 2.3	24.2 ± 1.1

observed (Table 1). The influence of dissolved HSA could possibly be due to the solubilizing effect of the protein leading to a reduced adsorption of mTHPP to HSA nanoparticles. At low HSA concentrations (0.75 and 1.0%) a high variability of the mTHPP loading was found (Table 1). This is indicative for a slight instability of the mTHPP nanoparticle mixtures. Based on these results a higher concentration of 1.5% dissolved HSA was routinely used for further loading experiments. At this concentration a high particle loading could be combined with stable particle formulations. For mTHPC a nearly constant loading with increasing amounts of dissolved HSA was achieved (Table 2).

3.4. Influence of incubation time and pH value on loading procedure

The influence of the incubation time on the photosensitizer loading was evaluated at a concentration of 1.5% of dissolved HSA for mTHPP and a concentration of 2.0% for mTHPC. For investigation of the pH dependency of the drug load a concentration of 1.5% dissolved HSA was used for both photosensitizers. In the pH range of 5–10 no significant influence on the mTHPP adsorption to HSA nanoparticles was observed (Fig. 2). The binding efficiency of mTHPC showed a significant decrease with increasing pH. At pH 5 a slight instability of the suspension was observed leading to an aggregation of the nanoparticles.

The variation of the incubation time between 0.5 and 24 h revealed no influence on the binding of both photosensitizers to the nanoparticles (data not shown). Due to the fast process of adsorption short incubation times of 0.5 h were sufficient for a reproducible mTHPP and mTHPC loading to HSA nanoparticles.

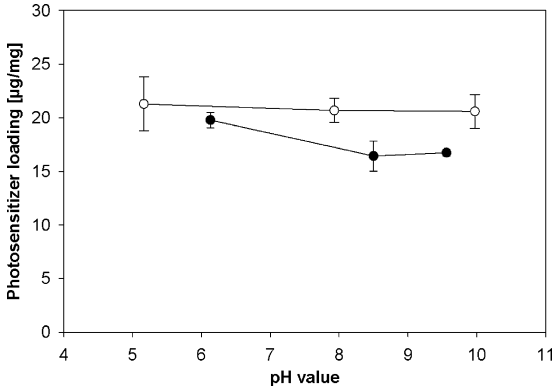

Fig. 2. Drug loading of HSA nanoparticles with mTHPP (○) and mTHPC (●) depending on the pH value in the range of 5–10 (mean ± S.D.; $n = 3$).

Based on these results further drug loading experiments were performed at pH 8.0 for mTHPP and pH 7.0 for mTHPC in combination with short incubation times of 1 h leading to a reproducible photosensitizer binding to HSA nanoparticles.

3.5. Electron microscopic characterization of photosensitizer loaded nanoparticles

Drug loaded HSA nanoparticles were characterized via scanning electron microscopy (SEM) in order to exclude photosensitizer precipitation in the reaction mixture during nanoparticle loading. Nanoparticles were prepared on membrane filtration units in order to enable a rapid sample drying without particle aggregation. SEM

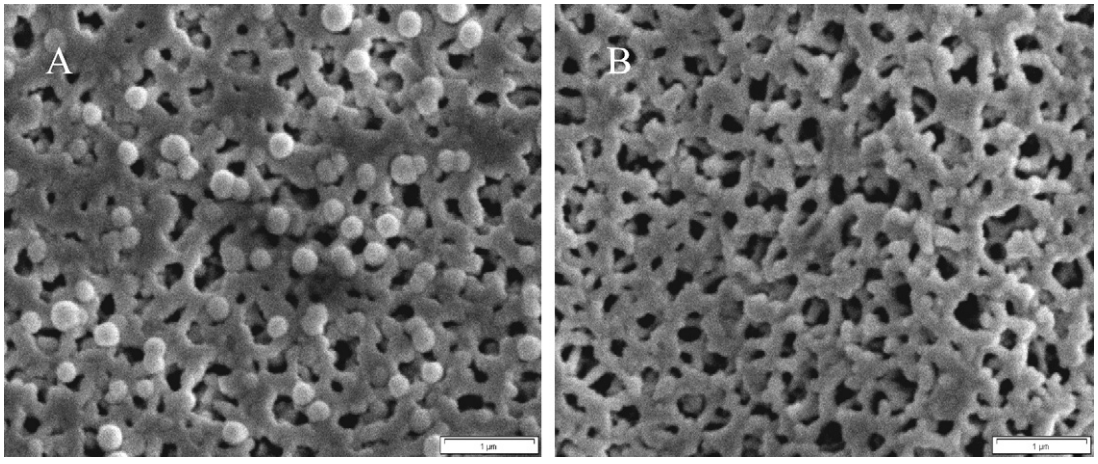

Fig. 3. Scanning electron microscopy (SEM) of (A) mTHPC loaded HSA nanoparticles prepared in the presence of 1.5% dissolved HSA in ethanol 34.3% (v/v) for drug adsorption process and (B) empty membrane filter units (water) used for sample preparation.

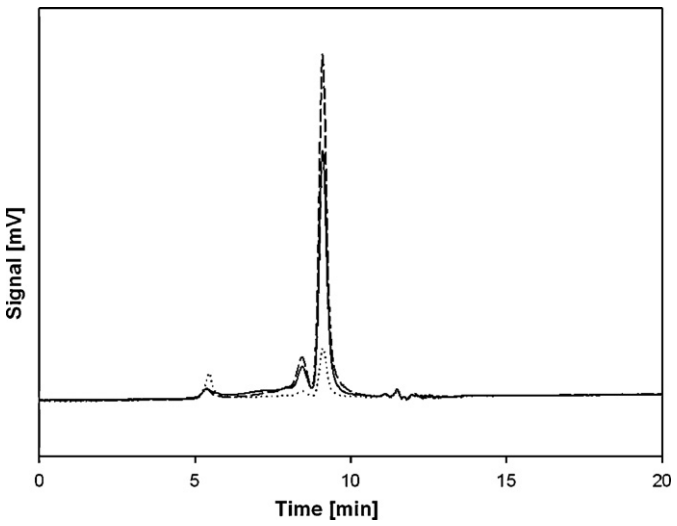

Fig. 4. SEC chromatograms of the supernatant of mTHPC loaded HSA nanoparticles (2.0% HSA) after the first centrifugation step (. . .), a standard containing no nanoparticles but dissolved HSA and mTHPC in hydroethanolic solution (- - -), and HSA in aqueous solution (—).

revealed only well defined spherical HSA nanoparticles of expected size and polydispersity. No crystalline structures of precipitated mTHPC were observed (Fig. 3).

3.6. Protein adsorption to HSA nanoparticles

The SEC chromatograms show a decrease of the HSA concentration from 65.02 μg/mL for a hydroethanolic standard solution containing mTHPC and HSA to 12.36 μg/mL in the supernatant of the HSA nanoparticles which indicates that HSA is easily adsorbed by HSA nanoparticles (Fig. 4). A control sample containing HSA in purified water was measured under comparable conditions.

3.7. Zeta potential measurements of mTHPC and mTHPP loaded nanoparticles

The zeta potential of mTHPC and mTHPP loaded nanoparticles was measured as well as of unloaded HSA nanoparticles. There was no significant change in the zeta potential over the whole time storage for both drug formulations and the unloaded colloid system (Fig. 5).

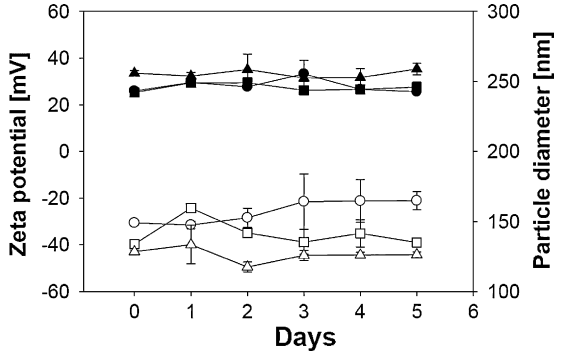

Fig. 5. Zeta potential (white) and particle diameter (black) measurements of mTHPP (■) and mTHPC (●) loaded nanoparticles and of the unloaded particle system (▲) over 5 days of storage. The loading was performed in the presence of 1.5% (m/v) of dissolved HSA for mTHPP and 2.0% for mTHPC.

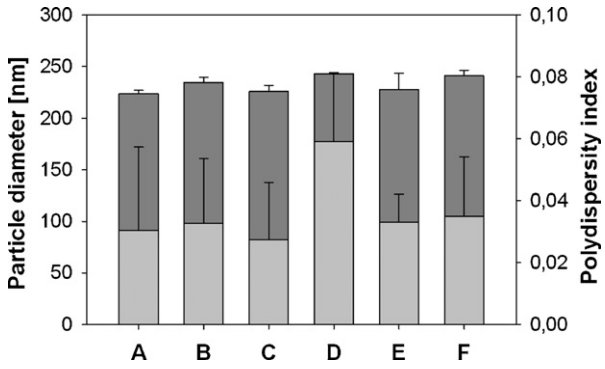

Fig. 6. Size ( ) and polydispersity ( ) index of mTHPC loaded HSA nanoparticles in aqueous suspension containing 3% of sucrose after 1 day (A), 3 weeks (C), and 6 weeks (E) of storage. Samples freeze dried in the presence of 3% sucrose after storage over 1 day (B), 3 weeks (D), and 6 weeks (F) followed by resuspension in purified water (mean ± S.D.; $n = 3$).

3.8. Freeze drying of mTHPC loaded HSA nanoparticles

A freeze drying method for the mTHPC loaded HSA nanoparticles was established using 3% (m/v) of sucrose as stabilizer according to an earlier study by Anhorn et al. (2008). The freeze dried samples were stored over 6 weeks at room temperature without any significant change (ANOVA) in particle size or polydispersity after redispersion with water (Fig. 6). Although the aqueous nanoparticle suspension showed no instability over the same period of time the freeze dried samples are assumed to have the advantage of a better long-term stability.

3.9. Photophysical characterization of mTHPP and mTHPC loaded nanoparticles

As can be seen from Fig. 7, the absorption spectrum of mTHPP in ethanol consists of one strong absorption peak caused by $S_0 \rightarrow S_{n>2}$ (B or Soret band) transitions in the blue region (380–430 nm). Besides Soret band, four weak Q bands caused by two $S_0 \rightarrow S_1$ (Qx bands) and two $S_0 \rightarrow S_2$ (Qy bands) transitions are observed in the red region. The maximum of the Soret band of mTHPP locates at

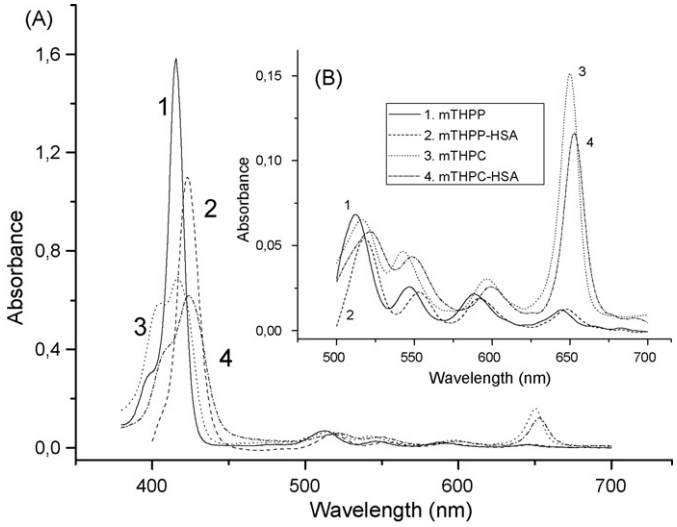

Fig. 7. Absorption spectra of mTHPP, mTHPC in ethanol as well as mTHPP and mTHPC loaded HSA nanoparticles in water. (A) Whole UV–vis region and (B) Q bands region. The absorption extinction is scattering corrected. (1) Solid line: mTHPP; (2) dashed line: mTHPP loaded HSA nanoparticles; (3) dotted line: mTHPC, and (4) dashed dotted line: mTHPC loaded HSA nanoparticles.

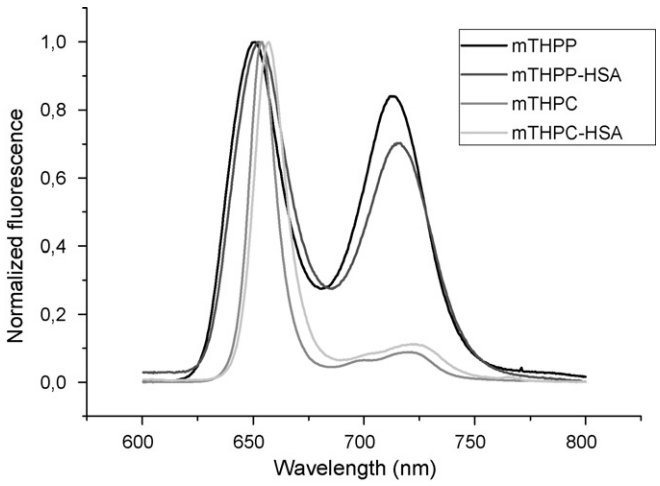

Fig. 8. Steady-state fluorescence of mTHPP, mTHPC as well as mTHPP and mTHPC loaded HSA nanoparticles. The fluorescence intensities are normalized. (1) Black: mTHPP; (2) dark gray: mTHPP loaded HSA nanoparticles; (3) Gray: mTHPC, and (4) light gray: mTHPC loaded HSA nanoparticles.

415 nm, while the Soret band of mTHPP loaded HSA nanoparticles exhibits a bathochromic shift to 423 nm. The centres of the four Q bands of mTHPP locate at 512, 546, 589, and 645 nm, respectively. Their counterparts for mTHPP loaded HSA nanoparticles are 517, 552, 592, and 648 nm.

mTHPP binding to HSA nanoparticles results in a reduced absorption in the Soret band region (about 70%) compared to that of mTHPP (Fig. 7) when scattering is considered. On the contrary, the absorption in the Q band region is very similar to that of mTHPP.

The *absorption spectra* of mTHPC and mTHPC loaded HSA nanoparticles also show the typical behaviour of metal free porphyrins. Due to the degeneration of one double bond, the chlorin mTHPC has a stronger absorption in the Qx (0, 0) band than the porphyrin mTHPP. The extinction coefficient of mTHPC at 650 nm is around 53,000 mol^{-1} cm^{-1}, which means 12 times higher than that of mTHPP (Fig. 7B).

The shapes of the fluorescence spectra of mTHPP and mTHPP loaded HSA nanoparticles look very similar (Fig. 8). The maximum of the $S_{1,0} \rightarrow S_{0,0}$ transition of mTHPP loaded HSA nanoparticles slightly shifts to 653 nm compared to that of mTHPP at 650 nm. The fluorescence peak of the $S_{1,0} \rightarrow S_{0,1}$ transition also shifts from 713 to 716 nm compared to that of mTHPP. The ratio of the intensities of two fluorescence peaks of $S_{1,0} \rightarrow S_{0,1}$ transition to $S_{1,0} \rightarrow S_{0,0}$ transition of mTHPP loaded HSA decreases to 0.69 compared to 0.84 of mTHPP. The quantum yield of fluorescence emission from the mTHPP loaded HSA nanoparticles resembles that of mTHPP.

For mTHPC, the fluorescence maximum of the $S_{1,0} \rightarrow S_{0,0}$ transition is at 654 nm. This peak shifts to 657 nm for mTHPC loaded HSA nanoparticles. The peak of the $S_{1,0} \rightarrow S_{0,1}$ transition can be seen as a fluorescence shoulder in the spectra of mTHPC and mTHPC loaded HSA nanoparticles. The fluorescence emission intensity of the $S_{1,0} \rightarrow S_{0,1}$ transition of mTHPC is lower than that of mTHPP. The fluorescence quantum yield of mTHPC loaded HSA nanoparticles in water is reduced to 30% compared to that of mTHPC in ethanol.

The fluorescence decay curves of mTHPP loaded HSA nanoparticles and mTHPC loaded HSA nanoparticles can be fitted with three fluorescence lifetimes (Table 3). For mTHPP loaded HSA nanoparticles, the longest component t_1 is 8.2 ns, which is similar to that of the mTHPP monomers (9.6 ns). Such a slightly shortened lifetime has been reported for photosensitizers attached to large units, for instance, pheophorbide a coupled to dendrimers (Hackbarth et al., 2005). The amplitude of τ_1 exceeded 40% of the total fluorescence intensity of mTHPP loaded HSA nanoparticles. At the same time, the decay time τ_2 with 2.1–2.3 ns shows an amplitude of about 25%. The shortest lifetime τ_4 (0.35 ns) contributes with 32.9% to the whole fluorescence signal.

The longest component τ_1, which relates to monomers, was not observed for mTHPC loaded HSA nanoparticles. Lifetimes τ_4, τ_3 and τ_2 contribute with 60, 30 and 10% to the total fluorescence of mTHPC loaded HSA nanoparticles, respectively.

Triplet state lifetime of photosensitizer τ_T, *singlet oxygen luminescence lifetime* τ_Δ and singlet oxygen quantum yield of mTHPP as well as mTHPC loaded HSA nanoparticles were calculated by fitting the singlet oxygen luminescence decay curves. The results are shown in Table 4. The triplet lifetime (τ_T) of water-soluble photosensitizer Rose Bengal in D_2O is 3.3 μs.

The *triplet lifetimes* of mTHPP and mTHPC loaded HSA nanoparticles in D_2O are 24.9 and 20.0 μs, respectively. The triplet lifetime of mTHPP and mTHPC in ethanol is 0.31 and 0.23 μs, respectively, which is much shorter than that of mTHPP and mTHPC loaded HSA nanoparticles.

The *singlet oxygen* generated by mTHPP and mTHPC loaded HSA nanoparticles in D_2O has quite a long lifetime. The lifetime was calculated to be 65 μs for mTHPP loaded HSA nanoparticles and 66 μs for mTHPC loaded HSA nanoparticles (Table 4), respectively, while the well-known value of singlet oxygen lifetime in D_2O is around 68 μs. Our measurement of singlet oxygen generated by Rose Bengal in D_2O gave a lifetime of 64 μs, which is in a good agreement with Ogilby and Foote (1983).

At the same time, the singlet oxygen quantum yields (Φ_Δ of mTHPP and mTHPC loaded HSA nanoparticles are very low (0.03 for both samples)). On the contrary, mTHPP and mTHPC have quite high singlet oxygen quantum yields in ethanol of about 0.63 and 0.65, respectively.

3.10. Singlet oxygen measurement in Jurkat cells

It was previously reported that photosensitizer loaded HSA nanoparticles were accumulated in Jurkat cells followed by an effective decomposition in the cellular lysosomes (Chen et al., 2009). Therefore, the singlet oxygen generation was analysed in this lymphocytic cell system. After 5 h of incubation with mTHPP, mTHPC, mTHPP and mTHPC loaded HSA nanoparticles, respectively, the singlet oxygen luminescence decay curves from inside Jurkat cells were measured (Fig. 9). The obtained parameters are: the singlet oxygen lifetime τ_Δ generated by mTHPP in cells is 0.85 μs and the triplet lifetime τ_T = 3.5 μs. The τ_Δ of mTHPP loaded

Table 3
Fluorescence lifetime τ of mTHPP, mTHPC in ethanol and mTHPP loaded HSA nanoparticles, mTHPC loaded HSA nanoparticles in aqueous suspension.

Samples	τ_1 [ns] ±0.2/[%]	τ_2 [ns] ±0.1/[%]	τ_3 [ns] ±0.1/[%]	τ_4 [ns] ±0.05/[%]	χ^2
mTHPP in EtOH	9.6/[100]	–	–	–	1.01
mTHPP loaded HSA nanoparticles	8.2/[41.6]	2.3/[25.5]	–	0.35/[32.9]	1.02
mTHPC in EtOH	8.6/[100]	–	–	–	1.04
mTHPC loaded HSA nanoparticles	–	2.2/[10.5]	0.7/[29.1]	0.12/[60.4]	1.07

Percentage contribution of lifetimes to total fluorescence presented in brackets.

Table 4
Singlet oxygen generation and triplet parameters of Rose Bengal, mTHPP, mTHPC as well as mTHPP and mTHPC loaded HSA nanoparticles in suspension and in Jurkat cells.

Samples	τ_T [μs] (in D_2O)	τ_Δ [μs] (in D_2O)	Φ_Δ (±0.03) (in D_2O)	τ_T [μs] (in Jurkat cells)	τ_Δ [μs] (in Jurkat cells)
Rose Bengal[a]	3.3 ± 0.1	64 ± 3	0.75	–	–
mTHPP[b]	0.31 ± 0.05	15.2 ± 0.5	0.63	3.5 ± 0.1	0.85 ± 0.05
mTHPP loaded HSA nanoparticles[a]	25 ± 1	65 ± 3	0.03	4.5 ± 0.1	1.10 ± 0.05
mTHPC[b]	0.23 ± 0.05	14.4 ± 0.3	0.65	3.7 ± 0.1	0.80 ± 0.05
mTHPC loaded HSA nanoparticles[a]	20 ± 1	66 ± 4	0.03	4.0 ± 0.1	0.55 ± 0.05

[a] Singlet oxygen measured in D_2O.
[b] Singlet oxygen measured in ethanol. Singlet oxygen measurement in cells: incubation time 5 h.

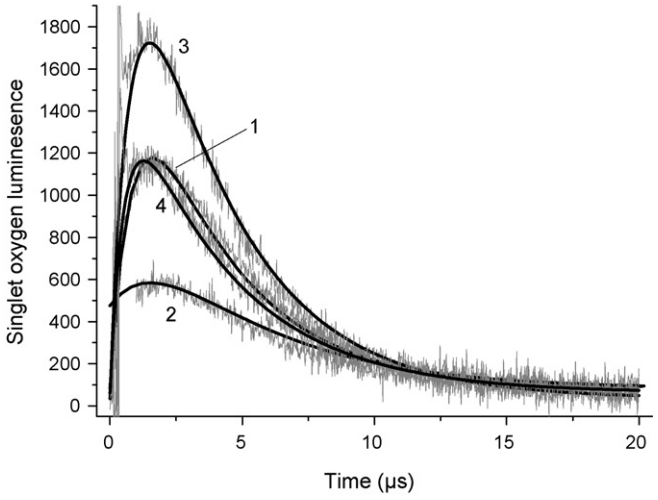

Fig. 9. Singlet oxygen luminescence decay curves in Jurkat cells incubated with mTHPP, mTHPC as well as mTHPP and mTHPC loaded HSA nanoparticles for 5 h (irradiation wavelength: 532 nm for mTHPP and mTHPP loaded HSA nanoparticles; 650 nm for mTHPC and mTHPC loaded HSA nanoparticles; illumination dose: 500 μW average power). Gray curves represent measuring data. (1) mTHPP; (2) mTHPP loaded HSA nanoparticles; (3) mTHPC; (4) mTHPC loaded HSA nanoparticles. Black thick smooth curves represent fitting curves.

HSA nanoparticles is 1.10 μs and τ_T = 4.5 μs (Table 4). The singlet oxygen generated by mTHPC and mTHPC loaded HSA nanoparticles showed a shorter lifetime which indicates interaction with the particle surface. For mTHPC, τ_Δ = 0.80 μs and τ_T = 3.7 μs. At the same time, for mTHPC loaded HSA nanoparticles, τ_Δ = 0.55 μs and τ_T = 4.0 μs.

The singlet oxygen quantum yields in cell suspension are difficult to determine since there is no reference for that. However, the singlet oxygen luminescence intensities of mTHPC and mTHPC loaded nanoparticles are higher than the intensities of mTHPP and mTHPP loaded nanoparticles, respectively (Fig. 9).

4. Discussion

Nanoparticle mediated drug delivery is a well established strategy to overcome side effects of cancer therapeutics (Konan et al., 2003; Wartlick et al., 2004; Balthasar et al., 2005). Regarding porphyrin derivates the risk of thromboembolic events or pain at the injection site can be reduced by the use of water based nanoparticulate preparations for parenteral application instead of organic solutions of the photosensitizers.

Biocompatible materials such as human serum albumin (HSA) play an important role in the development of new nanoparticulate formulations because of the good biodegradability of the resulting particle system. For the development of our drug carrier system a well established preparation method for HSA nanoparticles (Marty et al., 1978; Weber et al., 2000; Langer et al., 2003) was combined with the improved adsorption of two lipophilic photosensitizers in aqueous solution stabilized by the addition of HSA as a solubilizer for porphyrins. The binding of porphyrin derivatives to these nanoparticles was based on the known interaction of photosensitizers with protein solutions building complexes with bovine serum albumin (BSA) or lipoproteins (Sasnouski et al., 2005). Additionally, the aggregation of photosensitizers is a well known problem in the development of new formulations and it was previously shown that mTHPC shows strong aggregation in methanol/water mixtures containing more than 50% of water (Bonnett et al., 2001). Proteins such as albumin derivatives are known to inhibit aggregation and stabilize the monomeric form of the photosensitizer. On the other hand some disadvantages of adsorptive drug loading to nanoparticles have to be expected: the particle surface will be blocked for covalent modifications by drug targeting ligands and a fast release of the photosensitizers has to be anticipated.

For our adsorptive drug loading procedure preformed HSA nanoparticles were incubated with the photosensitizer in the presence of dissolved HSA in an ethanol/water mixture containing 34.3% (v/v) ethanol. On the one hand the chosen ethanol concentration prevents the precipitation of dissolved albumin in an unwanted desolvation process and on the other hand it increases the solubility of the photosensitizers in the medium. Under these conditions the addition of HSA was still necessary to stabilize the hydroethanolic photosensitizer solution (see Fig. 1).

The adsorption of dissolved HSA to HSA nanoparticles was investigated by SEC analysis. This was to strengthen the assumption that the improved loading rates are a result of photosensitizer adsorption to dissolved HSA followed by adsorption of this complex to HSA nanoparticles. Under the chosen conditions about 81% of the dissolved HSA was adsorptively attached to the preformed HSA nanoparticles.

After drug loading the particles were purified and were obtained as aqueous suspension. Under the aspect of further *in vivo* experiments a particle diameter between 150 and 300 nm in combination with a monodisperse size distribution was chosen. Particles smaller than 100 nm are well known to penetrate most tissues and have no selectivity for tumours while larger particles show a faster opsonization and elimination from the blood (Harashima et al., 1994).

For direct quantification of the photosensitizer in the purified formulations enzymatic degradation of the HSA nanoparticles was used. For pepsin a complete degradation of the prepared albumin nanoparticles was described within 30 min at a pH value of 1–3 (Langer et al., 2008). The quantification method showed that increasing concentrations of dissolved HSA led to a slight decrease in mTHPP binding to the nanoparticles. A drug binding efficiency of about 20 μg mTHPP per mg nanoparticles was achieved. For mTHPC a nearly constant loading ratio with increasing amounts of HSA was shown. A drug payload of 25 μg mTHPC per mg nanoparticle was obtained.

After drug loading nanoparticles without any change in size or polydispersity were obtained. The loading efficiency was independent of incubation time. Additionally, the influence of different pH values was investigated to optimize the loading process. We have expected that the effect of the pH value on the lipophilicity of photosensitizers (Cunderlikova et al., 2001) may influence the effi-

ciency of drug adsorption of both photosensitizers. Surprisingly, we observed no significant influence of the pH on mTHPP loading to HSA nanoparticles but an instability of the nanoparticle system at lower pH values. A pH value of 8.0 was found as the optimum for mTHPP loading because of the stability of the resulting nanoparticle system. In contrast a significant but mild influence of the pH value on binding efficiency of mTHPC was observed but instability of the particle system at lower pH values was a problem. A pH value of 7.0 was used as under these conditions a high loading rate in combination with particle stability could be achieved.

The stability of the systems was supported by scanning electron microscopy (SEM) and zeta potential measurements. In SEM no changes in the appearance of the used nanoparticles before and after drug loading were detectable and no signs of photosensitizer aggregates were observed besides drug loaded HSA nanoparticles. With regard to the zeta potential a slight increase from −40 to −30 mV caused by the drug adsorption process was observed for both carrier systems. These results indicate that the adsorption of the drugs caused changes of the surface structure of HSA nanoparticles. However, charge neutralization by drug loading never resulted in critical values bearing the risk of aggregation.

A freeze drying method for the mTHPC loaded nanoparticles was established in order to achieve a better long-term stability for this formulation. For parenteral formulations freeze drying is a standard method which protects the drug from biological contamination or hydrolysis (Anhorn et al., 2008). The resuspended HSA nanoparticles showed no changes in size or polydispersity index over storage time which indicates a stable nanoparticle suspension (Fig. 6). Samples of the same composition but without the addition of the stabilizer sucrose were used as control for these experiments. In the absence of sucrose the particles showed a strong aggregation and polydisperse size distribution after the freeze drying process (data not shown). On the other hand, the control samples containing the stabilizer and stored at 4 °C in aqueous suspension were stable over the period of storage (Fig. 6).

With regard to the photophysical properties the extinction in the absorption spectra of mTHPP and mTHPC loaded HSA nanoparticles still reached about 70% when compared to mTHPP and mTHPC in solution (Fig. 7). This illustrates that no strong photosensitizer aggregates formed during drug loading procedure.

The fluorescence quantum yield Φ_{FL} of mTHPP loaded HSA nanoparticles stays the same as fre mTHPP. However, Φ_{FL} of mTHPC loaded HSA nanoparticles decreased to 30% compared to free mTHPC. This correlates with their fluorescence lifetimes. The contribution of τ_1 is 40% of the total fluorescence, which presents mTHPP monomers (Table 3). However, τ_1 does not appear in mTHPC loaded HSA nanoparticle fluorescence, which indicates that no photosensitizer monomers exist in this particulate formulation. The shorter lifetimes are usually caused by interactions between photosensitizer molecules in limited heterogeneous microenvironment (Ambroz et al., 1994; Pfister et al., 2008).

The high singlet oxygen quantum yields Φ_{Δ} of mTHPP and mTHPC in ethanol (Table 4) decrease dramatically when attached to HSA nanoparticles ($\Phi_{\Delta} = 0.03$). At the same time, the singlet oxygen lifetime τ_D of mTHPP and mTHPC loaded HSA nanoparticles keeps the same value with Rose Bengal in D_2O. This indicates that the singlet oxygen is not quenched after generation. The low singlet oxygen quantum yield is caused by not only low local oxygen concentration in HSA nanoparticles but also by photosensitizer interactions (Bartlett and Indig, 1999).

The low oxygen concentration microenvironment is supported by the values of triplet lifetimes. As can be seen in Table 4, free photosensitizers have very short triplet lifetime τ_T both in aqueous solution (3.3 μs for Rose Bengal in D_2O) and in organic solvent (0.31 and 0.23 μs for mTHPP and mTHPC in ethanol, respectively). However, triplet lifetimes of photosensitizers in oxygen-depleted samples increase significantly since the deactivation process of triplet state photosensitizers via type II photosensitization oxygen concentration in this case is inefficient (Paul et al., 2003). The triplet lifetimes τ_T of mTHPP and mTHPC loaded HSA nanoparticles in air saturated samples are very long (25 μs for mTHPP and 20 μs for mTHPC loaded HSA nanoparticles), which are longer than τ_T of free mTHPP and mTHPC in ethanol. This indicates that the oxygen concentration in the microenvironment of HSA nanoparticles is insufficient.

Besides low local oxygen concentration, HSA binding and photosensitizer aggregation also decrease singlet oxygen quantum yields of mTHPP and mTHPC loaded HSA nanoparticles. Photosensitizers bound to HSA are well protected against oxygen quenching since the access of oxygen to photosensitizers is limited (Lang et al., 1998). The very low singlet oxygen quantum yields of HSA nanoparticle-bound photosensitizers give a benefit for photosensitizer delivery since mTHPP and mTHPC loaded HSA nanoparticles will protect tissue from unnecessary damage until the photosensitizer is released. The endocytotic uptake of these nanoparticles into the lysosomes of cancer cells were investigated and will be published in part II.

The capability of singlet oxygen generation by mTHPP and mTHPC loaded HSA nanoparticles inside living cells was proven. After 5 h incubation, singlet oxygen luminescence from both mTHPP and mTHPC loaded HSA nanoparticles inside Jurkat cells was observed. Unlike their extremely long triplet lifetimes τ_T in solution, the values of τ_T for mTHPP and mTHPC loaded HSA nanoparticles in cells are 4.5 and 4.0 μs after 5 h incubation. The τ_T for mTHPP and mTHPC in cells are 3.5 and 3.7 μs, respectively. This demonstrates a process of photosensitizer release from the nanoparticles. The triplet lifetimes of mTHPP and mTHPC loaded HSA nanoparticles become shorter since the energy transfer between photosensitizer and oxygen is more efficient after drug release, due to the changed environment with a higher local oxygen concentration than inside the nanoparticles. The degradation of the photosensitizer loaded nanoparticles in Jurkat cells followed by the release of their drug payload and the increasing singlet oxygen generation will be shown in part II of this publication.

5. Conclusion

Under the chosen conditions adsorption of both photosensitizers, mTHPP and mTHPC to HSA nanoparticles is an efficient strategy for drug loading. Dissolved HSA acting as a solubilizer for the porphyrin derivates is a useful tool to enhance the affinity of drugs to the preformed carrier system. Nanoparticles of a well defined size, polydispersity and drug loading efficiency were obtained.

Photosensitizers bound to HSA nanoparticles have extremely low singlet oxygen quantum yields in aqueous suspension. There are two reasons for this. First of all, the local oxygen concentration on the surface of HSA nanoparticles is insufficient. Secondly, the deactivation process of triplet state photosensitizer by oxygen is less efficient when hydrophobic dyes are aggregated. After 5 h of incubation in cells, when mTHPP and mTHPC are released from HSA nanoparticles, singlet oxygen is effectively generated inside living cells.

The low singlet oxygen quantum yield of mTHPP and mTHPC in the nanoparticle suspension brings an advantage to drug delivery since phototoxic activity of the formulation before degradation of the particle system and drug release can be avoided. The uptake and the lysosomal degradation of these drug carrier systems followed by singlet oxygen generation and apoptosis of the cancer cells were investigated. These results will be published in the second part of this publication and the differences between the developed formulations will be shown.

In summary, all of our results lead to the conclusion that we are able to create a stable nanoparticulate formulation of the photosensitizers mTHPP and mTHPC which protect these drugs from aggregation and oxidation processes until the particles are taken up by living cells and release their drug payload.

Acknowledgements

The authors want to acknowledge BMBF (Bundesministerium für Bildung und Forschung; project 0312026A) for financial support and Biolitec AG Jena for reagent supply.

References

Ambroz, M., MacRobert, A.J., Morgan, J., Rumbles, G., Foley, M.S., Phillips, D., 1994. Time-resolved fluorescence spectroscopy and intracellular imaging of disulphonated aluminium phthalocyanine. J. Photochem. Photobiol. B 22, 105–117.

Anhorn, M.G., Mahler, H.C., Langer, K., 2008. Freeze drying of human serum albumin (HSA) nanoparticles with different excipients. Int. J. Pharm. 363, 162–169.

Balthasar, S., Michaelis, K., Dinauer, N., von Briesen, H., Kreuter, J., Langer, K., 2005. Preparation and characterisation of antibody modified gelatin nanoparticles as drug carrier system for uptake in lymphocytes. Biomaterials 26, 2723–2732.

Bartlett, J.A., Indig, G.L., 1999. Effect of self-association and protein binding on the photochemical reactivity of triarylmethanes. Implications of noncovalent interactions on the competition between photosensitization mechanisms type I and type II. Photochem. Photobiol. 70, 490–498.

Bonnett, R., Djelal, B.D., Nguyen, 2001. Physical and chemical studies related to the development of m-THPC (FOSCAN (R)) for the photodynamic therapy (PDT) of tumours. J. Porphyr. Phthalocyan. 5, 652–661.

Bourdon, O., Laville, I., Carrez, D., Croisy, A., Fedel, P., Kasselouri, A., Prognon, P., Legrand, P., Blais, J., 2002. Biodistribution of meta-tetra(hydroxyphenyl)chlorin incorporated into surface-modified nanocapsules in tumor-bearing mice. Photochem. Photobiol. Sci. 1, 709–714.

Brown, S.B., Brown, E.A., Walker, I., 2004. The present and future role of photodynamic therapy in cancer treatment. Lancet Oncol. 5, 497–508.

Chen, K., Preuß, A., Hackbarth, S., Wacker, M., Langer, K., Röder, B., 2009. Novel photosensitizer-protein nanoparticles for photodynamic therapy: photophysical characterization and in vitro investigations. J. Photochem. Photobiol. B 96, 66–74.

Compagnin, C., Bau, L., Mognato, M., Celotti, L., Miotto, G., Arduini, M., Moret, F., Fede, C., Selvestrel, F., Rio Echevarria, I.M., Mancin, F., Reddi, E., 2009. The cellular uptake of meta-tetra(hydroxyphenyl)chlorin entrapped in organically modified silica nanoparticles is mediated by serum proteins. Nanotechnology 20, 345101.

Cramers, P., Ruevekamp, M., Oppelaar, H., Dalesio, O., Baas, P., Stewart, F.A., 2003. Foscan uptake and tissue distribution in relation to photodynamic efficacy. Br. J. Cancer 88, 283–290.

Cunderlikova, B., Bjorklund, E.G., Pettersen, E.O., Moan, J., 2001. pH-dependent spectral properties of HpIX, TPPS2a, mTHPP and mTHPC. Photochem. Photobiol. 74, 246–252.

D'Cruz, A.K., Robinson, M.H., Biel, M.A., 2004. mTHPC-mediated photodynamic therapy in patients with advanced, incurable head and neck cancer: a multicenter study of 128 patients. Head Neck 26, 232–240.

Detty, M.R., Gibson, S.L., Wagner, S.J., 2004. Current clinical and preclinical photosensitizers for use in photodynamic therapy. J. Med. Chem. 47, 3897–3915.

Dougherty, T.J., Gomer, C.J., Henderson, B.W., Jori, G., Kessel, D., Korbelik, M., Moan, J., Peng, Q., 1998. Photodynamic therapy. J. Natl. Cancer Inst. 90, 889–905.

Greish, K., 2007. Enhanced permeability and retention of macromolecular drugs in solid tumors: a royal gate for targeted anticancer nanomedicines. J. Drug Target. 15, 457–464.

Hackbarth, S., Ermilov, E., Röder, B., 2005. Interaction of pheophorbide a molecules covalently linked to DAB dendrimers. Opt. Commun. 248, 295–306.

Harashima, H., Sakata, K., Funato, K., Kiwada, H., 1994. Enhanced hepatic uptake of liposomes through complement activation depending on the size of liposomes. Pharm. Res. 11, 402–406.

Henderson, B.W., Dougherty, T.J., 1992. How does photodynamic therapy work? Photochem. Photobiol. Sci. 55, 145–157.

Jux, N., Röder, B., 2010. The porphyrin handbook. In: Kadish, K.S., Guilard, R. (Eds.), Targeting Strategies for Tetrapyrrole-based PDT. Academic Press.

Konan, Y.N., Chevallier, J., Gurny, R., Allemann, E., 2003. Encapsulation of p-THPP into nanoparticles: cellular uptake, subcellular localization and effect of serum on photodynamic activity. Photochem. Photobiol. 77, 638–644.

Kratz, F., 2008. Albumin as a drug carrier: design of prodrugs, drug conjugates and nanoparticles. J. Control. Release 132, 171–183.

Lang, K., Kubat, P., Mosinger, J., Wagnerova, D.M., 1998. Photochemical consequences of porphyrin and phthalocyanine aggregation on nucleoprotein histone. J. Photochem. Photobiol. A 119, 47–52.

Langer, K., Balthasar, S., Vogel, V., Dinauer, N., von Briesen, H., Schubert, D., 2003. Optimization of the preparation process for human serum albumin (HSA) nanoparticles. Int. J. Pharm. 257, 169–180.

Langer, K., Anhorn, M.G., Steinhauser, I., Dreis, S., Celebi, D., Schrickel, N., Faust, S., Vogel, V., 2008. Human serum albumin (HSA) nanoparticles: reproducibility of preparation process and kinetics of enzymatic degradation. Int. J. Pharm. 347, 109–117.

Levy, J.G., 1995. Photodynamic therapy. Trends Biotechnol. 13, 14–18.

Marty, J.J., Oppenheim, R.C., Speiser, P., 1978. Nanoparticles—a new colloidal drug delivery system. Pharm. Acta Helv. 53, 17–23.

Matsumura, Y., Maeda, H., 1986. A new concept for macromolecular therapeutics in cancer chemotherapy: mechanism of tumoritropic accumulation of proteins and the antitumor agent smancs. Cancer Res. 46, 6387–6392.

Miele, E., Spinelli, G.P., Tomao, F., Tomao, S., 2009. Albumin-bound formulation of paclitaxel (Abraxane ABI-007) in the treatment of breast cancer. Int. J. Nanomed. 4, 99–105.

Moreno-Aspitia, A., Perez, E.A., 2005. Nanoparticle albumin-bound paclitaxel (ABI-007): a newer taxane alternative in breast cancer. Future Oncol. 1, 755–762.

Ogilby, P.R., Foote, C.S., 1983. Chemistry of singlet oxygen. 42. Effect of solvent, solvent isotopic substitution and temperature on the lifetime of singlet molecular oxygen. J. Am. Chem. Soc. 105, 3423–3430.

Oleinick, N.L., Morris, R.L., Belichenko, I., 2002. The role of apoptosis in response to photodynamic therapy: what, where, why, and how. Photochem. Photobiol. Sci. 1, 1–21.

Paul, A., Hackbarth, S., Mölich, A., Luban, C., Oelckers, S., Böhm, F., Röder, B., 2003. Comparative study of the photosensitization of Jurkat cells in vitro by pheophorbide-a and a pheophorbide-a diaminobutane poly-propylene-imine dendrimer complex. Laser Phys. 13, 22–29.

Pfister, A., Zhang, G., Zareno, J., Horwitz, A.F., Fraser, C.L., 2008. Boron polylactide nanoparticles exhibiting fluorescence and phosphorescence in aqueous medium. ACS Nano 2, 1252–1258.

Rancan, F., Helmreich, M., Molich, A., Jux, N., Hirsch, A., Roder, B., Witt, C., Bohm, F., 2005. Fullerene–pyropheophorbide a complexes as sensitizer for photodynamic therapy: uptake and photo-induced cytotoxicity on Jurkat cells. J. Photochem. Photobiol. B 80, 1–7.

Redmond, R.W., Gamlin, J.N., 1999. A compilation of singlet oxygen yields from biologically relevant molecules. Photochem. Photobiol. 70, 391–475.

Sasnouski, S., Zorin, V., Khludeyev, I., D'Hallewin, M.A., Guillemin, F., Bezdetnaya, L., 2005. Investigation of Foscan interactions with plasma proteins. Biochim. Biophys. Acta 1725, 394–402.

Schlothauer, J., Hackbarth, S., Röder, B., 2008. A new benchmark for time-resolved detection of singlet oxygen luminescence—revealing the evolution of lifetime in living cells with low dose illumination. Laser Phys. Lett., 1–6.

Steinhauser, I.M., Langer, K., Strebhardt, K.M., Spankuch, B., 2008. Effect of trastuzumab-modified antisense oligonucleotide-loaded human serum albumin nanoparticles prepared by heat denaturation. Biomaterials 29, 4022–4028.

Wartlick, H., Spankuch-Schmitt, B., Strebhardt, K., Kreuter, J., Langer, K., 2004. Tumour cell delivery of antisense oligonucleotides by human serum albumin nanoparticles. J. Control. Release 96, 483–495.

Weber, C., Coester, C., Kreuter, J., Langer, K., 2000. Desolvation process and surface characterisation of protein nanoparticles. Int. J. Pharm. 194, 91–102.

Zeisser-Labouebe, M., Lange, N., Gurny, R., Delie, F., 2006. Hypericin-loaded nanoparticles for the photodynamic treatment of ovarian cancer. Int. J. Pharm. 326, 174–181.

Zensi, A., Begley, D., Pontikis, C., Legros, C., Mihoreanu, L., Wagner, S., Buchel, C., von Briesen, H., Kreuter, J., 2009. Albumin nanoparticles targeted with Apo E enter the CNS by transcytosis and are delivered to neurones. J. Control. Release 137, 78–86.

Zhao, B., Yin, J.J., Bilski, P.J., Chignell, C.F., Roberts, J.E., He, Y.Y., 2009. Enhanced photodynamic efficacy towards melanoma cells by encapsulation of Pc4 in silica nanoparticles. Toxicol. Appl. Pharmacol. 241, 163–172.